SPECIFIC ION EFFECTS ON THE COMPLEXATION BETWEEN HYALURONIC ACID AND CHITOSAN

by
Sezin Mamaşoğlu
B.S., Chemistry, Boğaziçi University, 2021

Submitted to the Institute for Graduate Studies in
Science and Engineering in partial fulfillment of
the requirements for the degree of
Master of Science

Graduate Program in Chemistry
Boğaziçi University
2025

ACKNOWLEDGEMENTS

First and foremost, I would like to express my deepest gratitude to my advisor Assoc. Prof. Ayşe Başak Kayıtmazer for her inspiring mentorship, continuous support and her guidance throughout my academic journey. Her profound knowledge and critical insights helped me to successfully navigate the challenges I experienced.

I would also like to acknowledge my thesis committee members, Prof. A. Levent Demirel and Prof. Nihan Nugay, for giving their valuable time and thoughtful evaluations.

I would like to express my gratitude to my colleagues and friends in the Kayıtmazer Research Group, but especially but mostly to Esra Baydar for her spirit of friendship and emotional support which made even the most challenging days pleasant. To Gökçe Kantarcı, for her guidance on essentials of the ITC when I just started. I owe a gratitude also for Fatma Akçay Oğur for generously sharing her valuable insights and for bringing positivity to the lab, İlayda Akbulut for the enjoyable moments and support. And, I'm grateful to İbrahim Yusuf Keleş for his support in helping me start this journey and for all the fun we shared along the way.

I would like to thank to the research students of our group that I had the chance to mentor and work with throughout this journey for their curiosity and youthful energy: Rana, Aleyna, Ertuğrul, Sena, Melani, Ceyhan, Başak, Zeynep, Elif, Miray, İnci and Sevda.

Many thanks also all the members of Acar Research Group, Ayşenur, Halenur, Göknil, Nazlıcan, Ayşe Zeynep, Hüseyin, Elif, Hakan and Atakan for bringing energy and helping me to find a healthy balance between working hard and having good time.

Lastly, my sincere thanks go to my family and friends for their endless patience, encouragement and support throughout this journey. Their understanding and constant presence made the challenges more manageable. Thank you for always being there, reminding me to stay positive even at the toughest times.

This project was supported by TÜBİTAK Short-Term R&D Funding Program (Project Code: 120Z865).

ABSTRACT

SPECIFIC ION EFFECTS ON THE COMPLEXATION BETWEEN HYALURONIC ACID AND CHITOSAN

Complex coacervation is a liquid-liquid phase separation caused by the interaction of oppositely charged macromolecules and the entropy gain by counter-ions' release. Coacervation is shown to be influenced by a number of variables, including temperature, pH, ionic strength, the concentration and molecular mass of polymers, the charge density of polyelectrolytes, and the stoichiometry of the mixture. The understanding of interactions between the ions and polymers goes back to Hofmeister series based on ability of ions to precipitate proteins. The specific ion effects have also been studied for other biomacromolecules and polymers. Considering the ability to affect the stability and behavior of coacervates formed by charged polymers, the ion effects are therefore noteworthy in the context of complex coacervation. In this study, the impact of this series on the complexation and coacervation of hyaluronic acid (HA) with chitosan (CHI) at acidic pH has been investigated by light microscopy, turbidimetric titration, potentiometric titration and isothermal titration calorimetry (ITC) experiments. Light microscopy images were taken to demonstrate that the HA/CHI system formed coacervates. Turbidimetric titration experiments were utilized to investigate the coacervation process as a function of different salt types. The degree of ionization of HA and CHI was determined by potentiometric titration experiments. Isothermal titration calorimetry is applied to investigate the ion effects on the thermodynamics of HA/CHI complexation. Cation effects were investigated using chloride salts, whereas anion effects were investigated using sodium salts. Enthalpy values showed less change with monovalent cations whereas the enthalpy of complexation was found as more exothermic for magnesium ion than that of calcium ion. Acetate ion shows more exothermic enthalpy values compared to nitrate and chloride ions. The interactions between the two polyelectrolytes has the highest, most negative enthalpy values in the absence of salt.

ÖZET

SPESİFİK İYONLARIN HİYALÜRONİK ASİT VE KİTOSAN ARASINDAKİ KOMPLEKSLEŞME ÜZERİNDEKİ ETKİSİ

Kompleks koaservasyon, zıt yüklü makromoleküllerin etkileşimi ve karşı iyonların salınmasıyla entropi kazancının neden olduğu bir sıvı-sıvı faz ayrımıdır. Koaservasyonun sıcaklık, pH, iyonik kuvvet, polimerlerin konsantrasyonu ve moleküler kütlesi, polielektrolitlerin yük yoğunluğu ve karışımın stokiyometrisi dahil olmak üzere bir dizi değişkenden etkilendiği gösterilmiştir. İyonlar ve polimerler arasındaki etkileşimlerin anlaşılması, iyonların proteinleri çökeltme yeteneğine dayanan Hofmeister serisine kadar uzanır. Bu spesifik iyon etkileri şu anda diğer biyomakromoleküller ve polimerler için de incelenmektedir. Yüklü polimerler tarafından oluşturulan koaservatların stabilitesini ve davranışını etkileme yeteneği göz önüne alındığında, iyon etkileri bu nedenle kompleks koaservasyon bağlamında dikkate değerdir. Bu çalışmada, bu serinin asidik pH'da hiyalüronik asit (HA) ile kitosan (CHI) kompleksleşmesi ve koaservasyonu üzerindeki etkisi ışık mikroskobu, türbidimetrik titrasyon, potansiyometrik titrasyon ve izotermal titrasyon kalorimetrisi (ITC) deneyleri ile incelenmiştir. HA / CHI sisteminin koaservat oluşturduğunu göstermek için ışık mikroskobu görüntüleri alınmıştır. Farklı tuz türlerinin bir fonksiyonu olarak koaservasyon sürecini gözlemlemek için türbidimetrik titrasyon deneyleri kullanılmıştır. HA ve CHI'nin iyonlaşma derecesi, potansiyometrik titrasyon deneyleri ile belirlenmiştir. HA/CHI kompleksleşmesinin termodinamiği üzerindeki iyon etkileri izotermal titrasyon kalorimetrisi ile incelenmiştir. Katyon etkileri klorür tuzları kullanılarak, anyon etkileri ise sodyum tuzları kullanılarak araştırılmıştır. Entalpi değerleri tek değerlikli katyonlarla daha az değişiklik gösterirken, kompleksleşme entalpisi magnezyum iyonu için kalsiyum iyonundan daha ekzotermik olarak bulunmuştur. Asetat iyonu, nitrat ve klorür iyonuna kıyasla daha fazla ekzotermik entalpi değerleri göstermiştir. HA-CHI arasındaki etkileşimler tuz yokluğunda en yüksek, en negatif entalpi değerlerine ulaşmıştır.

TABLE OF CONTENTS

LIST OF FIGURES

LIST OF TABLES

LIST OF SYMBOLS

C_{inj}	Concentration of the HA
I_{total}	Total ionic strength of the medium
K	Binding coefficient
K_a	Binding constant
M_t	Concentration of CHI in the cell after titration with HA
M_t^o	Concentration of CHI
n	Binding stoichiometry
n_{coac}	Stoichiometry of maximum coacervate formation
n_{IP}	Stoichiometry of ion-pairing
V_o	Volume of the cell
X_t	Concentration of the HA in the cell after injection
α	Degree of ionization for HA
α_{coac}	Width of the Gaussian curve at half its peak value
β	Degree of ionization for CHI
ΔG	Change in Gibbs free energy
ΔG_{IP}	Gibbs free energy of ion pairing
ΔH	Change in enthalpy
ΔH_{BiB}	Enthalpy of buffer into buffer solution titration
ΔH_{BiC}	Enthalpy of buffer into CHI titration
ΔH_{coac}	Change in enthalpy of coacervation
ΔH_{dil}	Total enthalpy of dilution
ΔH_{HiB}	Enthalpy of HA into buffer solution titration
ΔH_{HiC}	Enthalpy of HA into CHI titration
ΔH_{IP}	Change in enthalpy of ion-pairing
ΔS	Change in entropy
ΔS_{IP}	Entropy change of ion pairing
ΔV	Volume of HA injected into the cell
% T	Percent transmittance
100 - % T	Turbidity

LIST OF ACRONYMS/ABBREVIATIONS

BiB	Injection of buffer into buffer solution
BiC	Injection of buffer into CHI
BLG	β-lactoglobulin
BSA	Bovine serum albumin
CHI	Chitosan
CS	Chondroitin sulfate C
DD	Degree of deacetylation
HA	Hyaluronic acid
HiB	Injection of HA into buffer solution
HiC	Injection of HA into CHI solution
ITC	Isothermal titration calorimetry
PANa	Poly(sodium acrylate)
PDADMAC	Poly(diallyldimethylammonium chloride)
PGlu	poly(L-glutamic acid sodium salt)
PMETAC	poly(2-(methacryloxy)ethyl)trimethylammonium chloride)
PO	poly(L-orthine hydrobromide)
PSPMA	potassium poly(3-sulfopropylmethacrylate)
PSS	pol-(p-styrene sulfonate)
PTMA	poly-(trimethylammonium-2-ehtylmethylacrylate)

1. INTRODUCTION

1.1. Coacervation

Complex coacervation is a liquid-liquid phase separation caused by the interaction of oppositely charged macromolecules, leading to a dense coacervate phase that coexists with a dilute supernatant phase.[1-3] Bungenberg de Jong and Kruyt first studied this phenomenon by showing that coacervation is an effective method to concentrate polymers from dilute solutions.[4] Furthermore, Oparin hypothesized that the droplets of coacervates act as precursors to the first living cells. [5]

This physical phenomenon can take place in two ways: it may occur from a uniform aqueous solution, known as simple coacervation, or from the interaction of one or more oppositely charged macroions - such as polyelectrolytes, proteins, and colloids - resulting in complex coacervation.[2, 6-8] The latter is primarily driven by two driving forces: the intermolecular electrostatic interactions, a type of non-covalent interaction, and the entropy gain by counter-ions' release. It is important to note that other driving forces may also be contributing to complex coacervation, including hydrophobic interactions and hydrogen bonding. [9-11]

There has been significant interest in complex coacervation within various application areas such as encapsulation[12-14], protein purification[15], tissue engineering[16], drug delivery[17, 18], adhesives, and coatings.[19] Furthermore, thanks to its bioactive properties complex coacervates have been used for 3D bioprinting. [20]

Coacervation is influenced by several variables, including pH, ionic strength, temperature, polymer concentration, molecular weight, charge density, and the mixture stoichiometry.[21] Kayitmazer and her co-workers [21] investigated the complex coacervation of hyaluronic acid and chitosan, emphasizing the influence of pH, charge density, ionic strength, chain length, and charge ratio on their phase behavior.

Notable findings indicate coacervation is non-stoichiometric and the phase separation is favored with higher charge density of chitosan and longer hyaluronic acid chain length.

To better understand the parameters driving coacervation, Du et al. [22] studied the role of some key parameters (ionic strength, pH, charge of the polyelectrolyte, and protein charge distribution) regarding polysaccharide-protein coacervation of hyaluronic acid (HA) with bovine serum albumin (BSA) or β-lactoglobulin (BLG) system. Based on how the charges on the protein are distributed, BSA or BLG can interact with charged polymer HA, where any variation in ionic strength or pH results in a change in charges on both HA and proteins thus altering the strength of the protein-polyelectrolyte interaction. They correlated the charge anisotropy of protein and ionic strength to the critical pH values to gain insight into the formation of complexes, coacervation or precipitation. They also did a thermodynamic analysis by isothermal titration calorimetry (ITC) on HA-BSA and HA-BLG samples, demonstrating the higher affinity in the former interaction.

Effect of ionic strength which was investigated in polyelectrolyte-protein and polyelectrolyte-polyelectrolyte systems has also been studied for protein-protein complex coacervation. For example, Hachfi et al.[23] investigated lactoferrin/β-lactoglobulin complex coacervation by focusing on the effect of ionic strength with different NaCl concentrations. Binding energy measured by ITC is found to be promoted at the lower concentrations of added NaCl, however, at 20 mM and higher NaCl concentrations the phase separation is found to be disfavored.

One notable example of salt effects on polyelectrolyte coacervation involves the study by Perry et al.[24] who investigated how the formation of coacervation between two vinyl polyelectrolytes was affected by different types of salts. They observed higher turbidity up to a certain salt concentration, in which further addition diminished the interactions between the two polyelectrolytes, indicated by a decrease in turbidity. They also found that coacervate formation was disfavored in the presence of divalent salts such as $CaCl_2$ and Na_2SO_4 compared to the monovalent salt NaCl where the turbidity vs salt concentration plot shows lower critical salt concentration (the point at which no phase separation is detectable) for the former. However, per unit of ionic strength, higher critical salt concentration was found for Na_2SO_4 than NaCl and $CaCl_2$. This result can be explained

by the fact that SO_4^{2-}, being kosmotropic, promote phase separation by decreasing the polymer solubility. Moreover, when they examined the anion effects of CH_3COO^-, Cl^- and NO_3^- they observed that kosmotropic CH_3COO^- showed higher critical salt concentration, whereas turbidity plots of Cl^- and NO_3^- showed negligible variation. Additionally, for the cation effects, chloride salts of Na^+, K^+, Mg^{2+}, Ca^{2+}, ranking of the critical salt concentration is observed to follow Hofmeister ordering with lowest for chaotropic Ca^{2+} and highest for kosmotropic K^+.

1.2. Specific Ion Effects

The understanding of interactions between the ions and polymers goes back to Franz Hofmeister's study in 1888.[25, 26] His classification of the ions based on their ability to precipitate proteins has led to the development of the Hofmeister series, aka specific ion effects. Ions are categorized as kosmotropes and chaotropes. The strongly hydrated kosmotropic ions are located on the left side of the series, stabilize proteins, and promote salting-out behavior. However, weakly hydrated chaotropic ions on the right side of the series destabilize the proteins and promote salting-in behavior. This phenomenon is not limited to proteins, it can similarly be investigated on the scope of macromolecules, polymers, and colloids.[27-30] Nevertheless, the interpretation of interactions of ions with macromolecules has yet to be fully understood. These interactions, indeed, are more sophisticated than corresponding interactions involved in proteins.

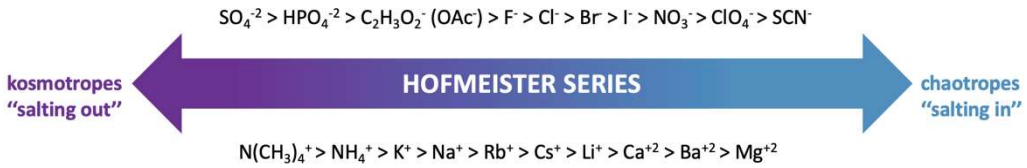

Figure 1.1. The series of Hofmeister anions and cations.[31-34]

In general, the specific ion effects are more evident for anions than cations. The typical order of the anions and cations is given in Figure 1.1.[31-34] Cl^- and Na^+ are the two ions that typically divide the series for the anions and cations, respectively. Kosmotropes have larger hydration radii and have more interactions with water molecules,

so they are less mobile compared to the weakly hydrated smaller chaotropic ions.[35] However, the ordering of the ions can be altered due to some parameters such as pH and salt concentration which causes the ions to follow different sequences. For instance, a study done by Oppermann and Schulz [36] found that the enthalpy of complexation between two oppositely charged polyelectrolytes of poly-(p-styrene sulfonate) (PSS) and poly(trimethylammonium-2-ethylmethacrylate) (PTMA) showed less change with monovalent cations. The enthalpy values change between -0.68 to -1.70 kJ/mol for the following conditions: Rb^+, Cs^+, K^+, Na^+, and Li^+.

Zhang and Cremer [37] investigated the anion effects on the phase transition of lysozyme by monitoring the change in could-point temperature. They observed a direct Hofmeister series effect of anions at higher salt concentrations, but a reverse order was followed at lower salt concentrations.

Tatini et al.[38] studied the specific ion effects on the rheological and thermal behavior of polysaccharide-based biopolymers by investigating the change in hydration properties, chain interactions, and viscosity. The study revealed that the responses of the neutral polysaccharide guar gum and negatively charged sodium hyaluronate to the added salts are different. The viscosity of the guar gum is affected according to the direct Hofmeister effect, where the viscosity of the dispersion with Na_2SO_4 is highest and that of $NaClO_4$ is lowest. For sodium hyaluronate, the reverse trend is observed. Thus, they highlighted the importance of hydration and the charge of polymers in determining the effect of ions. The polymer network of the guar gum is strengthened with enhanced interchain interactions by the dehydration effect of kosmotropes. However, the negatively charged sodium hyaluronate chains, which compete with kosmotropic ions for water molecules, lose some of their water molecules that form the hydration layer around the chains, leading to an increase in the intrapolymer repulsion between charged carboxyl groups of HA.

Das and Majumdar [39] studied the electrostatic effect of two kosmotropic, two chaotropic salts and their mixtures on swelling, drug release profile, and rheological properties of gelatin-alginate hydrogels. They mentioned that water binds more strongly to the ions with the ability to rearrange water (kosmotropes) than the ions which disturb the

structure of water (chaotropes). Chaotropic anions, having smaller hydration radius with greater mobility, enhance the charge screening within gelatin chains via diffusing themselves into the polymer. Whereas kosmotropes exhibit less charge screening with their larger hydrodynamic radius and lower mobility. Therefore, when kosmotropes are present, amines of the gelatin chains are more positively charged that can make more interactions with the negatively charged alginate. In the presence of kosmotropic anions (SO_4^{-2} and CH_3COO^-) electrostatic interactions between the two polymers is strengthened due to less charge screening which results in a better release profile and lower swelling degree. However, the formation of hydrogen bonding is favored by chaotropes with more charge screening, thus enhanced self-healing properties of the prepared hydrogel.

In a recent study by Zhu et al. [40] how the microenvironment of biomolecular condensates changes in response to the presence of ions was reported. They discussed the changes in micropolarity, linked to dielectric constant variations (the increase of which is associated with the increase in micropolarity), and the microviscosity. The quantification of these two terms was done by utilizing fluorescence lifetime imaging microscopy with two different probes. The fluorescence lifetime of polarity-sensitive probe decreases with higher micropolarity, whereas the lifetime of rotor-based probe increases with increasing microviscosity. To understand formation of intrinsically disordered protein condensates, this study investigated two types of model systems: elastin-like and resilin-like polypeptides. They used NaSCN, Na_2SO_4, NH_4Cl and GdnHCl salts, where the two strongest salting-out ions are represented by NH_4^+ and SO_4^{2-}, while Gdn^+ and SCN^- serve as salting-in ions. The findings highlight that the microenviroment of the condensate is affected by salting-in (SCN^-) and salting-out (SO_4^{2-}) anions differently. The micropolarity of condensate is increased by SCN^- raising the water fraction in the protein-rich region. However, micropolarity is reduced in the presence of SO_4^{2-} and hydration of proteins is lowered which facilitates interactions between the elastin-like polypeptides. The micropolarity of resilin-like polypeptide condensates decreased and microviscosity increased at higher SO_4^{2-} (salting-out ion) concentrations which was attributed to the possible formation of salt bridges or electrostatic cross-linking. In the case of NH_4^+ at concentrations below 1 M, micropolarity is increased with increasing salt concentration due to its shielding effect on electrostatic interactions between the two aminoacids. However, at higher concentrations, micropolarity decreases. Meanwhile, an opposite trend

is observed for microviscosity. As a result, they concluded that salting-in ions promote cosolvation and increase micropolarity while reducing microviscosity through association with protein backbone.

1.3. Hyaluronic Acid and Chitosan

In this study, specific ion effects on the complexation between the two oppositely charged biopolyelectrolytes, where hyaluronic acid (HA) as a polyanion and chitosan (CHI) as a polycation were studied. The linear carbohydrate polymer HA has carboxylic groups on its monomers (D-glucuronic acid and N-acetyl glucosamine) deprotonation of which leads to negatively charged functional groups on the chain. Chitosan, also a linear polysaccharide, consists of N-acetyl-D-glucosamine and D-glucosamine units derived from the deacetylation of chitin. Protonation of the amine groups in its structure makes it a positively charged polyelectrolyte. Thus, its degree of chitosan deacetylation (DD) and pH of the medium have an effect on its charge density.[41] Increasing the DD leads to higher charge density, containing higher number of NH_3^+ groups in its monomers. [42, 43] There are wide range of applications of chitosan and hyaluronic acid in tissue engineering and drug delivery thanks to their structure and biodegradability, and biocompatibility.[44-47]

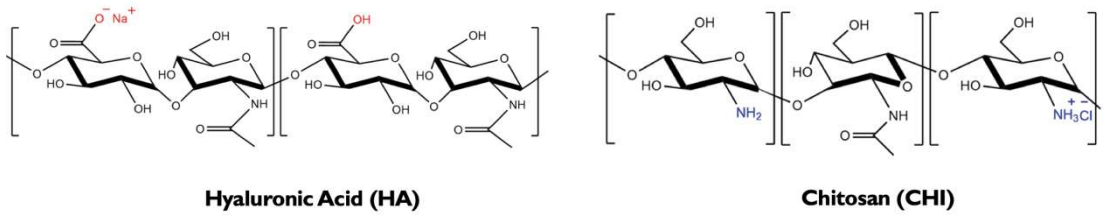

Figure 1.2. Chemical structures of HA and CHI.

1.4. Isothermal Titration Calorimetry (ITC)

Isothermal titration calorimetry (ITC) is an analytical technique used to study the thermodynamics of molecular interactions by monitoring the heat exchanged between the two interacting molecules and maintaining the temperature difference at zero between the sample and reference cell. [48]

The sample cell, reference cell, and syringe are the main components of the ITC instrument. One of the binding species is loaded into the sample cell, and the other one is titrated into it from a stirring syringe. In general, water or buffer in interest is present in the reference cell. During the titration process, small aliquots of the titrant solution are injected into the molecule of interest in the sample cell coated by an isothermal environment, providing a thermal equilibrium. According to the heat release or absorption at each successive injection, the instrument detects a decrease or increase in power to maintain a constant temperature difference, respectively. The power data converted from the temperature difference between the cells is displayed as raw data over time. Then, it is integrated to compute the heat change of interaction of each injection as a function of the molar ratio. After using fitting models to fit this enthalpy vs molar ratio data, thermodynamics parameters of binding stoichiometry (n), binding coefficient (K), change in Gibbs free energy (ΔG) and entropy (ΔS) can be obtained where the change in enthalpy (ΔH) is directly measured.[49, 50]

Since the ITC instrument does not require any additional experimental setup, such as chemical labels to the molecules of interest, it is a preferred method for studying the wide range of biomolecular interactions and complex systems. [51]

Vitorazi et al.[52] examined the thermodynamics of poly(diallyldimethylammonium chloride) (PDADMAC) / poly(sodium acrylate) (PANa) titrations at different concentrations, pH, and molecular weights together with changes in mixing order. They recognized the interaction between these two oppositely charged polyelectrolytes is a two-step mechanism: formation of charged complexes and coacervate formation as a primary and secondary process, respectively. They observed that the secondary enthalpic peak is

enhanced at a higher molecular weight of PANa, and fully deprotonated PANa at a higher pH increases the binding enthalpy. Although differences in mixing orders lead to changes in the coacervation profile from exothermic to endothermic, there is no change in the polyelectrolyte complexes which shows an endothermic profile.

Dos Santos de Macedo et al.[53] studied the thermodynamic characteristics of the PDADMAC/sodium alginate system at varying pH values. They also investigated how thermodynamic parameters influence the layer formation of these two polyelectrolytes, to which they applied ITC. The ITC data with different sequences of titrations showed a two-step process. The first step of complexation is found to be entropically driven with positive enthalpy of binding values across experimental pH values and becomes less endothermic at lower pH values. Although the thermodynamic characteristics of the first step did not change with changing titration sequence, that of the coacervation step showed distinct behavior. In this step, the titration of PDADMAC to alginate exhibited an exothermic behavior, while the reverse titration was found to be endothermic.

To deepen the understanding of several factors affecting the coacervation, in our recent study [54] we investigated the thermodynamics of complexation and coacervation of two oppositely charged biopolyelectrolytes (HA and CHI) at various ionic strengths, pHs and molecular weights of HA using ITC together with the observations from light microscopy, turbidimetric titrations and zeta potential experiments. The HA/CHI mixture was observed to become an opaque solution with increase in turbidity when HA was titrated into CHI. The increase in opacity is attributed to the formation of a higher number of droplets at the higher molar ratios [HA]/[CHI]. The coacervation process was described to be nonstoichiometric with nonzero zeta potentials showing droplets carry a net charge. The apparent thermodynamics of complexation from ITC revealed that aforementioned factors had a major impact on energetics where the dominant factor for coacervation is found be entropy. The general trend of strengthening interactions with increasing pH was observed. Moreover, the stoichiometry of ion-pairing and entropic driving force for coacervation process showed a decrease with increasing ionic strength.

In the study by Yang et al.[55] specific ion effects of different sodium salts (NaCl, NaBr, NaI, NaAc, and $NaClO_4$) on the PSS/PDADMA complexes were investigated. In their study, they applied ITC to explore complexation enthalpy. They observed two distinct ΔH phases with varying salt concentrations: at a concentration of NaCl beyond 0.5 M the reduced enthalpy change is found compared to the phase at lower NaCl concentration where at both regimes the complex formation is exothermic. For the enthalpy of complexation, they reported the most exothermic value at NaAc condition -6.03 kJ/mole than NaCl with -2.8 kJ/mole. However, the remaining salts showed endothermic enthalpy change with 1.9, 3.2 and 12.8 kJ/mole for NaBr, NaI and $NaClO_4$, respectively.

The complex coacervation of oppositely charged PDADMAC and PSSNa was studied using ITC, focusing on the enthalpic and entropic driving forces by Fu et al.[1] They observed that entropy is the dominant factor for the coacervation of these two polyelectrolytes. During the complexation process that contribution comes from the counterion release and water molecules. Moreover, the enthalpic contributions of complexation is reduced in solutions with high ionic strengths where salt ions screen the charges, thus electrostatic interactions diminished. Additionally, the role of selected Hofmeister anions (Br^-, Cl^-, NO_3^-, ClO_3^-, Ac^- and F^-) as counter ions of PDADMAC on complexation was also investigated. The enthalpy of complexation values measured by ITC in the presence of these ions found to be negative, demonstrating the exothermic behavior. Finally, they highlighted that the release of more hydrated counterions plays role in increasing the entropy since they are more easily displaced during the complexation. In other words, more hydrated counterions have a strong affinity to water, and therefore have less affinity to stay bound to polyelectrolytes. Then the counterion release upon complexation of oppositely charged polyelectrolytes becomes higher in magnitude, which is accompanied with a higher entropy gain by the release of these counterions and water molecules.

1.5. Preliminary Studies

Coacervation of hyaluronic acid (HA) with chitosan (CHI) was previously studied in our group with respect to the effect of Hofmeister salts [56, 57]. However, that study did not involve the potentiometric titration experiments of HA and CHI. More importantly,

turbidimetric titration and ITC data were missing for the condition of pH = 3.25 and HA with 199 kDa. Moreover, only the enthalpy values for complexation could be determined by applying a trivial method of ITC data analysis, namely “summing method”[1] With the summing method, no information could be obtained about the thermodynamic parameters regarding ion-pairing and coacervation processes. In our current study, the HA-CHI coacervation is investigated at acidic pH (pH = 3.25) by light microscopy, turbidimetry, potentiometric titration and isothermal titration calorimetry (ITC) experiments. By analyzing the isotherms from the ITC results via a two-step model which was previously applied to study thermodynamics of oppositely charged polypeptides [9] and synthetics vinyl polymers [52, 53], the information about the thermodynamic parameters for both the ion-pairing and coacervation steps were obtained. The same salts as in the previous project (KCl, NaCl, $MgCl_2$, $CaCl_2$, $NaNO_3$ and NaOAc) were used in this project.

2. AIM OF THE STUDY

As mentioned in the introduction part of this thesis, coacervation is shown to be influenced by a number of variables, including temperature, pH, ionic strength, the concentration and molecular mass of polymers, the charge density of polyelectrolytes, and the stoichiometry of the mixture. Hofmeister series, aka specific ion effects, phenomenon has been investigated on the scope of macromolecules, polymers, polymers and colloids. Considering the ability to affect the stability and behavior of coacervates formed by charged polymers, the specific ion effects is therefore noteworthy in the context of complex coacervation.

Kayitmazer and her co-workers investigated the complex coacervation of hyaluronic acid and chitosan, emphasizing the influence of pH, charge density, ionic strength, chain length, and charge ratio on their phase behavior. Moreover, in our recent publication [54], the apparent thermodynamics of HA-CHI mixture was investigated by ITC as a function of ionic strength, pH and chain length. However, in the aforementioned publications, only NaCl is used as the type of salt. Therefore, further investigation is necessary to determine the effect of different salt ions.

Subsequent to these findings, the study mentioned in the Section 1.5 was conducted for HA-CHI system with different salts. However, the shortcomings of that study (no data analysis by a proper fitting method, no information regarding thermodynamic parameters of ion-pairing and coacervation processes) guided the current study.

Therefore, in this study, specific ion effects of different salts (KCl, NaCl, $MgCl_2$, $CaCl_2$, $NaNO_3$ and NaOAc) on the complexation and coacervation between the two oppositely charged biopolyelectrolytes, HA and CHI were studied at acidic pH = 3.25 with HA of 199 kDa by applying the modified two-step model of ITC data analysis.

3. EXPERIMENTAL SECTION

3.1. Materials

Dried sodium hyaluronate (HA) was purchased from Lifecore Biomedical (Chaska, MN, USA) with average molecular weight (M_w) of 199 kDa (Product #: HA200K, Lot #: 026564) (determined by viscosimetry).

Chitosan chloride (CHI) with molecular weight 396 kDa, determined from gel permeation chromatography, with 83% degree of deacetylation (Product No: 54039, Batch No: 313-130117-01) was purchased from Heppe Medical Chitosan GmbH (Halle, Germany).

Sodium chloride (NaCl, Product No: 106404), potassium chloride (KCl, Product No: 104936), and sodium acetate trihydrate ($NaOAc.3H_2O$, Product No:106267) were purchased from Merck (Darmstadt, Germany). Sodium nitrate ($NaNO_3$, Product No: 481757) and magnesium chloride hexahydrate ($MgCl_2.6H_2O$, Product No: 459337) were purchased from Carlo Erba (Milano, Italy). Calcium chloride dihydrate ($CaCl_2.2H_2O$, Product No: 909026) was purchased from ISOLAB Chemicals (Eschau, Germany). Citric acid (99%, Product No: C0759)

The dialysis membrane, which was a SnakeSkin™ tubing with a molecular weight cut-off (MWCO) of 3500 g/mol (Product No: 68035) was purchased from Thermo Scientific™ (Massachusetts, USA). Solutions were filtered using 0.45 μm cellulose acetate HPLC syringe filters (Product No: 56133345, 56253345), which were purchased from Labmarker (Istanbul, Turkiye).

Research-grade pH 2.00, 4.00, 7.00, and 10.00 buffer solutions used for pH-meter calibration (Product No: 908.B02, 908.B04, 908.B07 and 908.B10, respectively), NaOH and HCl solutions (0.1N and 1 N) used for pH adjustments, methanol used for ITC washing module (liquid chromatography grade, Product No: 947.047.2501) were purchased from ISOLAB Chemicals (Wertheim, Germany). All experiments were done with Milli-Q grade water (resistivity of 18.2 MΩ·cm) obtained from PURELAB Quest system (ELGA Veolia, UK).

3.2. Methods

3.2.1. Dialysis for Counterion Exchange

75 ml of polyelectrolyte solutions containing either 0.5 mg/ml HA or 0.5 mg/ml CHI were prepared in Milli-Q water. HA was originally supplied with Na^+ counterions and CHI with Cl^- counterions. To exchange the counterions with the relevant Hofmeister ion, 0.1 M NaX or MCl_n salt solutions were prepared in Milli-Q water. For NaX solutions, X was Cl^-, OAc^- or NO_3^-, and for MCl_n solutions, M^{+n} was Mg^{+2}, Ca^{+2}, Na^+ or K^+. Counterion exchange of the polymer was done by placing the HA and CHI solutions with the original counterions into semi-permeable dialysis membranes (SnakeSkin™, MWCO: 3.5 kDa), and then placing the membranes in 5 L of the salt solutions. For example, the Na^+ counterion of HA was exchanged with Ca^{+2} by dialyzing it against 0.1 M $CaCl_2$ solutions. Dialysis of the polymers was done for three days against three separate batches of the salt solutions that were refreshed every 24 hours, followed by three additional days of dialysis in Milli-Q water, by refreshing water at 24-hour intervals.

The substitution of the counterions were confirmed by SEM-EDS analysis (FEI-Philips XL30 Environmental Scanning Electron Microscope with Field Emission Gun, equipped with EDAX-Energy Dispersive X-ray Analysis Unit) conducted at the Advanced Technologies Research and Development Center of Boğaziçi University.

3.2.2. Turbidimetric Titration

Buffered salt solutions were prepared by dissolving citric acid and corresponding salt in volumetric flask. The concentration of the citric acid was 5 mM in all cases. The pH of the solutions was adjusted to the desired pH = 3.25 ± 0.05 by using 0.1 N or 1 N NaOH, 0.1 N or 1 N HCl for all the salt solutions except for NaOAc, where glacial AcOH was used to adjust the pH. HA and CHI were individually dissolved in these salt solutions. The solutions were prepared by mixing for 2 h resulting in solutions of 0.5 mg /ml HA and 0.1 mg/ml CHI. Polymer solutions were then filtered with 0.45 μm cellulose acetate HPLC syringe filters prior to experiments. Under salted conditions, the total ionic strength (I_{total}) of the medium was 50 mM.

Turbidity measurements were performed by titrating 0.02 ml HA solution into the 2.6 ml CHI solution by adding increments of 4 µl for the first injection and 20 µl for the subsequent 19, under constant stirring, using a Brinkmann PC 950 colorimeter equipped with 420 nm filter at 25°C. The percent transmittance (% T) was recorded and converted to % Turbidity (100 - % T). The total number of additions and the titration intervals were kept the same as the ITC experiments. Reproducible results were obtained by repeated titrations of three separate runs.

3.2.3. Potentiometric Titration

The degree of ionization of HA and CHI in dependence on pH was determined by potentiometric titration experiments in 50 mM NaCl under nitrogen inert gas together with polymer-free control experiments. The pH of salt and polymer solutions were adjusted with 0.05 N, 0.1 N, 1 N NaOH and 0.05 N, 0.1 N, 1 N HCl. Prior to the experiments, the pH values of the polymers were fixed at 7.5 and 1.5 for HA and CHI, respectively. The degree of ionization value of HA is denoted by α and that of CHI by β. Modified Henderson-Hasselbalch equations were applied in order to drive α_{HA} and β_{CHI} values.[21]

3.2.4. Optical Light Microscopy

A drop of optical microscopy samples of HA/CHI mixtures at [HA]/[CHI] molar ratios of 0.16, 0.35 and 0.53 was taken and placed on the microscope slide and sealed with cover glass. Light microscopy images of the samples were obtained by using a Leica DMI 6000B Inverted Microscope equipped with a DFC295 camera at 20x magnification. Particle size analysis and monitoring of the evolution of coacervate droplets versus precipitates were done using the Leica Application Suite software, Version 3.8.0. A spherical particle was classified as a coacervate; otherwise, as a precipitate. 10 arbitrary spherical droplets at previously given [HA]/[CHI] molar ratios were selected in the field of observation, and then their diameters were measured by using a scale bar. Average particle sizes, together with the standard deviations, were reported from three replicates of each experiment.

3.2.5. Isothermal Titration Calorimetry (ITC)

ITC experiments were conducted using MicroCal ITC200 (Malvern Instruments, Malvern, UK). Polymer solutions were prepared at concentrations of 2.0 mg/ml for HA and 0. 4 mg/ml for CHI at the desired pH of 3.25 in 5 mM citric acid buffer, with ionic strength adjusted by the addition of the salt matching the counterion of the polymer; e.g. for studying the effect of $CaCl_2$, HA with Ca^{+2} counterions and CHI with Cl^- counterions were used. Prepared polymer samples were dialyzed with 3.5 kDa molecular weight cut-off (MWCO) semi-permeable membrane to eliminate buffer mismatching. During this process, the buffered salt solutions were refreshed every three hours for a total of five times. After dialysis, the polymer solutions were diluted with the remaining buffered salt solution of the last step to concentrations of 0.5 mg/ml HA and 0.1 mg/ml CHI, followed by a two-hour mixing period. Then, all samples were filtered with 0.45 μm cellulose acetate membranes and were degassed using ThermoVac degasser (Malvern Instruments, UK) to avoid bubble formation in the ITC cell and syringe. For all conditions, HA was titrated into CHI and the reference cell was filled with Milli-Q water. 20 successive injections of 2 μL HA (0.4 μL for the first injection, followed by 2 μL for each of the subsequent 19 injections) at intervals of 240s were used to titrate CHI, at a constant stirring rate at 310 rpm. The total enthalpy of dilution (ΔH_{dil}) was determined by carrying out three different experiments that consisted of injection of HA into buffer solution (HiB), buffer into CHI (BiC), and buffer into buffer solution (BiB). The net enthalpy of HA into CHI interaction (ΔH) was calculated by subtracting the total enthalpy of dilution (ΔH_{dil}) from the enthalpy of HA into CHI titration (ΔH_{HiC}) by applying

$$\Delta H = \Delta H_{HiC} - \Delta H_{dil} = \Delta H_{HiC} - (\Delta H_{HiB} + \Delta H_{BiC} - \Delta H_{BiB}). \quad (1.1)$$

3.2.6. ITC Data Fitting

The two-step model of Priftis et al.[9] was applied to fit the isotherms which describes the ion pairing and coacervation steps as formation of soluble complex and formation of polymer-rich liquid droplets, aka coacervation, respectively. Enthalpy versus molar ratio ([HA]/[CHI]) plots of HA to CHI titration after subtraction were used for fitting the data.

The [HA]/[CHI] molar ratio calculated from

$$\frac{[\mathrm{HA}]}{[\mathrm{CHI}]} = \frac{X_t}{M_t} \tag{1.2}$$

was determined by using the concentration of the HA in the cell after injection (X_t) expressed as

$$X_t = \frac{C_{inj}\,\Delta V}{V_o}\left(1 - \frac{\Delta V}{2V_o}\right) \tag{1.3}$$

and the concentration of CHI in the cell after titration with HA (M_t) described as

$$M_t = M_t^o\left(\frac{1-\frac{\Delta V}{2V_o}}{1+\frac{\Delta V}{2V_o}}\right) \tag{1.4}$$

where ΔV represents the volume of HA injected into cell, V_o is the volume of the cell, M_t^o is the concentration of CHI (material in the cell before injections), C_{inj} is the concentration of the HA (injectant).

Nonlinear least squares curve fitting with Excel Solver was done and total square of errors are minimized to obtain following parameters: n_{IP}, n_{coac}, ΔH_{IP}, ΔH_{coac}, K_a and α_{coac}, where n_{IP} represents stoichiometry of ion-pairing, n_{coac} stoichiometry of maximum coacervate formation, ΔH_{IP} and ΔH_{coac} represents change in enthalpy of ion-pairing and coacervation respectively, K_a is the binding constant and α_{coac} describes the width of the Gaussian curve at half its peak value. Then, Gibbs free energy (ΔG_{IP}) and the entropy change (ΔS_{IP}) of ion pairing are calculated from the following relationships $\Delta \mathrm{G} = -\mathrm{RT}\ln(K_a)$ and $\Delta G_{IP} = \Delta H_{IP} - T\Delta S_{IP}$. Average fitted values of the parameters, together with their standard deviation, were reported from the three replicates of each experiment.

4. RESULTS AND DISCUSSION

Firstly, the fundamental aim is to investigate the specific ion effects of NaCl, KCl, $CaCl_2$, $MgCl_2$, $NaNO_3$, and NaOAc salts on the formation of complex coacervation between hyaluronic acid and chitosan at acidic pH. The conditions for the experiments were based on preliminary work done in our lab in which the water-soluble salts with minimal toxicity were chosen that did not cause the HA-CHI mixture to precipitate. At I_{total} values equal to and higher than 100 mM, HA-CHI mixtures within salt solutions showed precipitation. Therefore, the total ionic strength of the system was kept at 50 mM. The working pH was selected as pH = 3.25 which is suitable to use since at higher pH values above (pH ≥ 6.5) chitosan is expected to precipitate.[58] In order to keep the pH of the medium constant at the chosen acidic condition the citric acid is chosen as a buffering agent, having pK_{a_1} = 3.13 at T = 25 °C.[59]

4.1. Turbidimetric Titrations

The effect of ions on the formation of complex coacervation of hyaluronic acid and chitosan was investigated in this study in the presence of the citric acid buffer with added salts, namely NaCl, KCl, $CaCl_2$, $MgCl_2$, $NaNO_3$, and NaOAc. The results of the turbidimetric titration experiments with all cations and anions together with the salt-free condition are given in Figure 4.1. During the titration process, formed coacervate droplets scatter the light and decrease the transmittance, leading to higher turbidity. Thus, higher turbidity of solution at a higher molar ratio indicates that a larger or higher number of droplets are formed reflected by higher light scattering observed at both plots in Figure 4.1.

The left graph shows the turbidity values for the selected chloride salts showing the effect of Na^+, K^+, Mg^{+2}, and Ca^{+2} cations. For all the cations, turbidity values increased with increasing ([HA]/[CHI]) molar ratio and order follows $K^+ > Na^+ > Mg^{+2} > Ca^{+2}$. Kosmotropic cations ($K^+$ and Na^+) show higher turbidity than chaotropic cations (Mg^{+2} and Ca^{+2}). So, it can be said that the order follows the Hofmeister series, except that Ca^{+2} comes after Mg^{+2}. These observations from the cation effects is consistent with the previous study done by Perry et al.[24] in which the ordering of critical salt concentration

(at which no detectable phase separation is observed) follows Hofmeister series with the lowest for chaotropic Ca^{2+} and highest for kosmotropic K^+ for the chloride salts of Na^+, K^+, Mg^{2+}, Ca^{2+}.

Figure 4.1(b) shows the turbidity values for the selected sodium salts, demonstrating the impact of Cl^-, OAc^- and NO_3^- anions. The observation in cations where turbidity increases at a higher molar ratio is also seen in the anions. The order of the turbidity values for the anions follows $Cl^- > NO_3^- > OAc^-$. The trend is more complex, where the relatively inert anion Cl^- (according to the salting in and out effects) shows higher turbidity compared to the kosmotropic OAc^-. The observed behavior of the ions in our system follow similar rationale to the finding of Yamazaki et al. [60] They reported that the order of the critical coagulation concentration, concentration that halved the turbidity, of the chitosan (CHI)/chondroitin sulfate C (CS) was highest for Cl^- followed by other relatively chaotropic ions where that of NO_3^- is also lower compared to Cl^-. They also calculated the electrostatic energy between the positively charged ammonium groups of CHI and CS, where the order shows the similar trend of $Cl^- > NO_3^-$, showing stronger interactions between polymers in the presence of kosmotropic ions. However, another study for a mixture of pAA and pAH showed that kosmotropic CH_3COO^- showed higher critical salt concentration, whereas turbidity plots of Cl^- and NO_3^- showed negligible variation. [24]

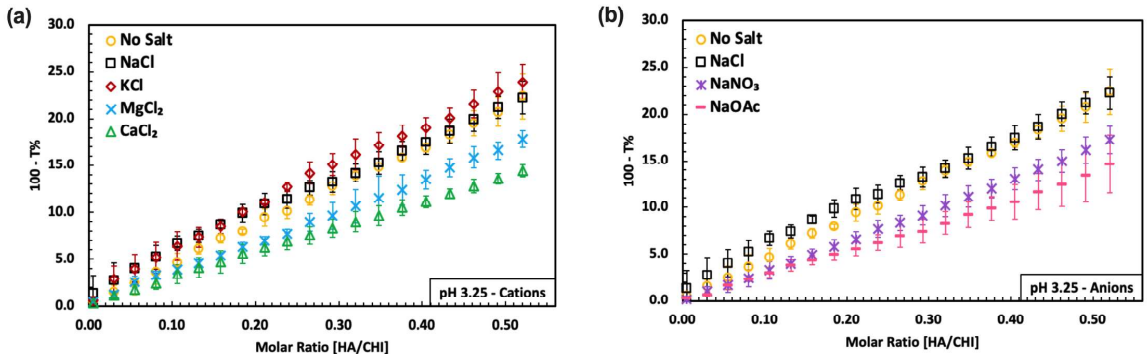

Figure 4.1. Turbidity (100 - %T) vs molar ratio ([HA]/[CHI]) plots for (a) cations (b) anions along with salt-free condition. All samples were prepared at pH = 3.25 in a citric acid/salt solution with I_{total}= 50 mM.

4.2. Optical Light Microscopy

For optical microscopy, a drop of HA/CHI mixtures at [HA]/[CHI] molar ratios of 0.16, 0.35, and 0.53 was taken during the turbidimetric titration experiments, and light microscopy images of the samples were obtained to observe the formation of coacervate droplets.

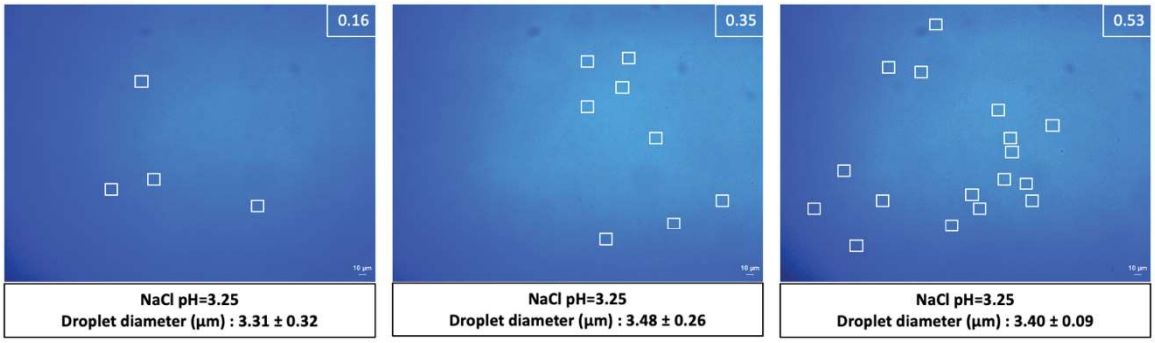

Figure 4.2. Light microscopy images of microdroplets of mixtures of 0.1 mg/mL $[CHI]_{init}$ and 0.5 mg/mL $[HA]_{init}$ at pH = 3.25, I_{total} = 50 mM at a molar ratio of [HA]/[CHI] = 0.16, [HA]/[CHI] = 0.35 and [HA]/[CHI] = 0.53.

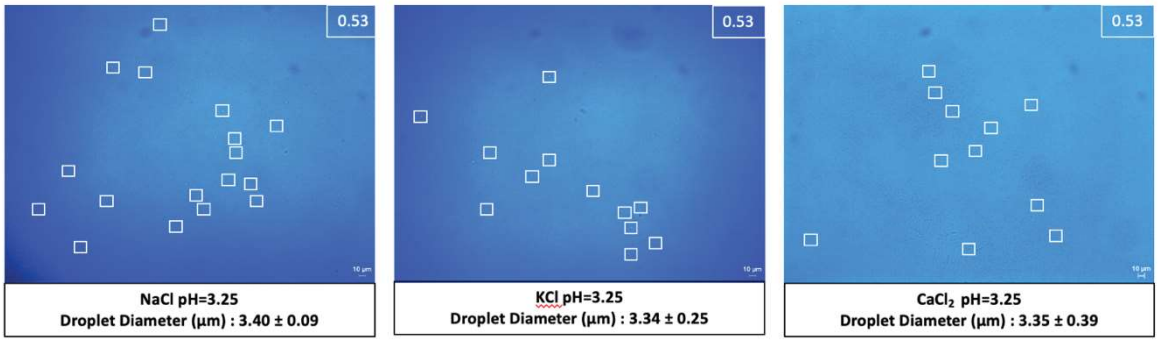

Figure 4.3. Light microscopy images of microdroplets of mixtures of 0.1 mg/mL $[CHI]_{init}$ and 0.5 mg/mL $[HA]_{init}$ at pH = 3.25, I_{total} = 50 mM at molar ratio of [HA]/[CHI] = 0.53.

Droplet diameter values at molar ratios of [HA]/[CHI] = 0.16, [HA]/[CHI] = 0.35 and [HA]/[CHI] = 0.53 are given for all the conditions in Figure 4.2 and Figure 4.4. As can be seen, droplet diameters are measured to be nearly the same among the three molar ratios. Thus, no correlation was found between the droplet sizes and the molar ratio of the HA/CHI mixture. Moreover, there is no significant difference found for the droplet diameters measured at the highest molar ratio of 0.53 where maximum coacervate droplet

formation is expected. The light microscopy images of HA/CHI mixture in KCl, NaCl and $CaCl_2$ solutions with citric acid buffer are given in Figure 4.3 to visualize the aforementioned observation.

However, a higher number of droplets were observed via light microscopy at the higher molar ratios, which may indicate the increase in turbidity values is born from more coacervate droplets formed. Light microscopy images of the NaCl condition at different molar ratios are given in Figure 4.2 as an example, showing the formation of more droplets at [HA]/[CHI] = 0.53 compared to [HA]/[CHI] = 0.35 and [HA]/[CHI] = 0.16. This validates the expectation that more phase separation occurs with greater number of [HA]/[CHI] droplets being formed.

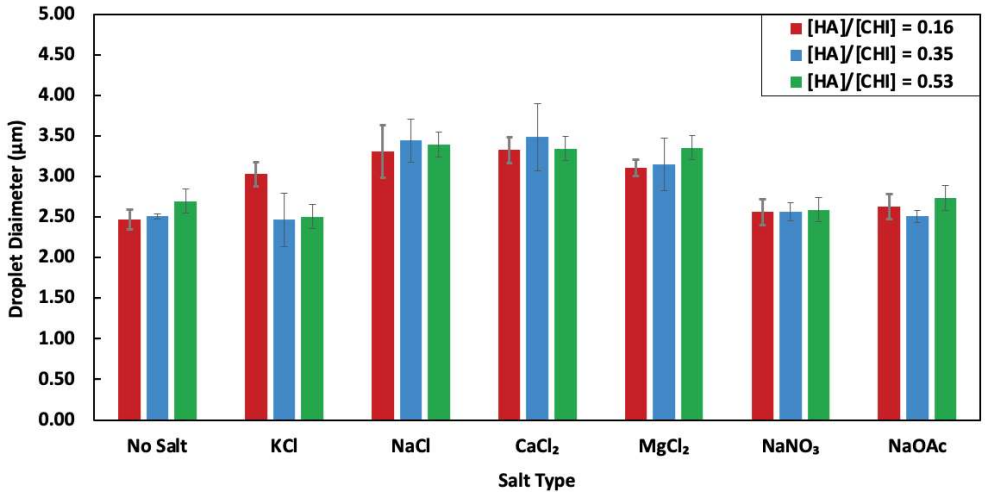

Figure 4.4. Droplet diameters obtained from the optical light microscopy images taken at the molar ratio of [HA]/[CHI] = 0.16, [HA]/[CHI] = 0.35 and [HA]/[CHI] = 0.53 in turbidimetric titration experiments.

4.3. Potentiometric Titration

The degree of ionization of HA and CHI was determined by potentiometric titration experiments in 50 mM NaCl under nitrogen inert gas together with polymer-free control experiments. The pH of salt and polymer solutions were adjusted with 0.05 N, 0.1 N, 1 N HCl and 0.05 N, 0.1 N, 1 N NaOH. The initial pH values for the polymers were fixed to 7.5 and 1.5 for HA and CHI, respectively. The degree of ionization value of HA is denoted by α and that of and CHI by β. Modified Henderson-Hasselbalch equations were applied in order to drive α_{HA} and β_{CHI} values.

The degree of ionization values of HA and CHI with respect to pH are given in Figure 4.5. As can be seen the degree of ionization of HA is decreased at lower pH values, whereas that of CHI increases. The HA chains were found to be 26 ± 0.02 % (α_{HA} = 0.26 ± 0.02) charged, and CHI chains are 99 ± 0.01 % charged (β_{CHI} = 0.99) at pH =3.25. Therefore, at this acidic pH value, CHI is nearly fully charged whereas HA is less charged in comparison.

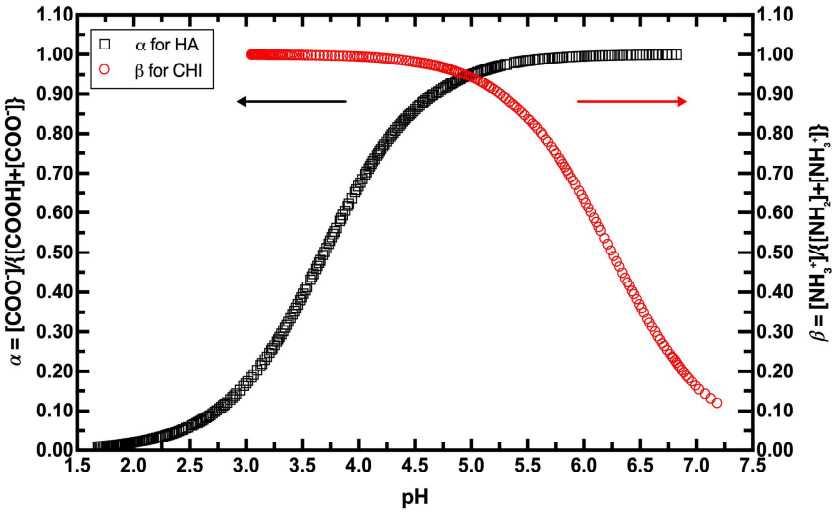

Figure 4.5. Potentiometric titration curves for HA (199 kDa) and CHI (396 kDa) in 50 mM NaCl.

4.4. Isothermal Titration Calorimetry

As previously mentioned in the Section 3.2.6, the modified two-step model was applied to fit the isotherms which describes the ion pairing and coacervation steps. The data fitting was done by nonlinear least squares curve fitting with Excel Solver to obtain following parameters: n_{IP}, n_{coac}, ΔH_{IP}, ΔH_{coac}, K_a and α_{coac}. This is done where total square of errors are minimized calculated by enthalpy values from the model subtracted from the experimental raw data. By examining the net enthalpy of HA into CHI interaction (experimental data after subtraction of dilutions), initial guesses for the aforementioned parameters were given and the best-fit results with the minimum total square of errors were found. Then, ΔG_{IP} and ΔS_{IP} of ion pairing are calculated from the following relationships $\Delta G = -RT \ln(K_a)$ and $\Delta G_{IP} = \Delta H_{IP} - T\Delta S_{IP}$. Average fitted values of the parameters, together with their standard deviation, were reported from the three replicates of each experiment.

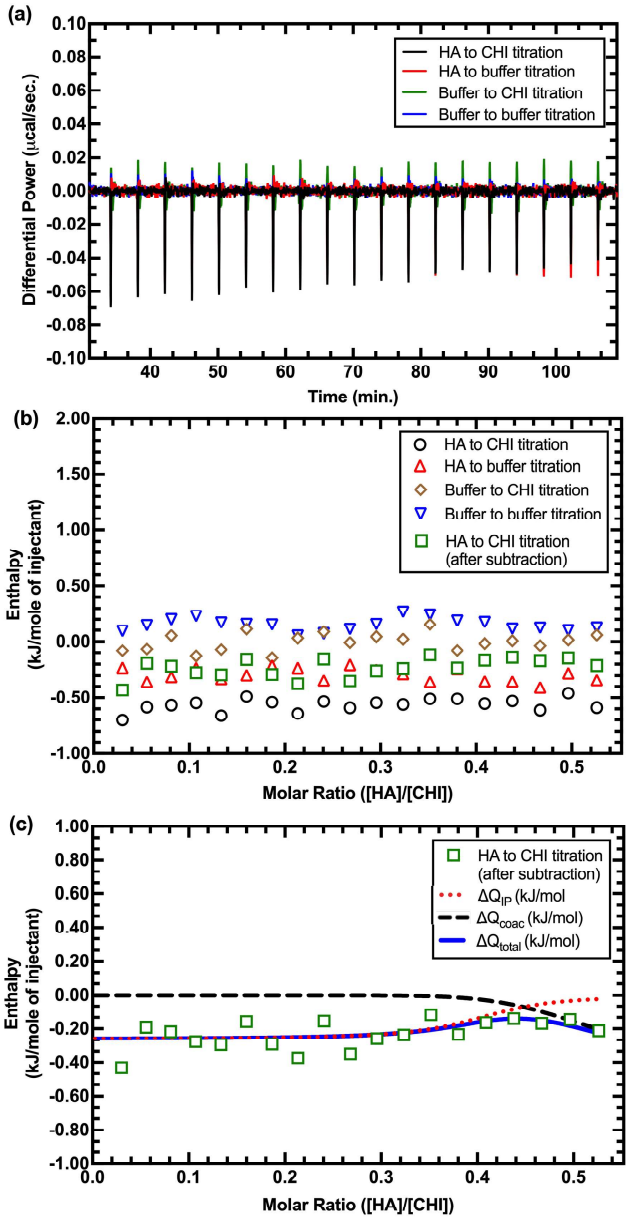

Figure 4.6. (a) Real-time thermogram of ITC experiments. (b) Enthalpy versus molar ratio ([HA]/[CHI]) plots for HA to CHI titration (○), HA to buffer titration (△), Buffer to CHI titration (◇), Buffer to buffer titration (▽) and HA to CHI titration after subtraction (□). (c) Fitted enthalpy curves of HA to CHI titration after subtraction (□), ion-pairing step (···), coacervation step (– –) and total enthalpy (—).

One representative ITC data set given in Figure 4.6 corresponds to the titration results at pH = 3.25 in citric acid/NaCl solution with I_{total} = 50mM, T = 25 °C. Raw enthalpy data is shown together with the fitted enthalpy curves with calculated ΔQ_{IP}, ΔQ_{coac} and ΔQ_{total} in Figure 4.6(c).

Table 4.1. Thermodynamic parameters of HA/CHI mixtures in citric acid buffer with added salts.

Salt Type	n_{IP}	n_{coac}	ΔH_{IP} (kJ/mol)	ΔH_{coac} (kJ/mol)	α_{coac}	K_a (L/mmol)	ΔG_{IP} (kJ/mol)	$-T\Delta S_{IP}$ (kJ/mol)
KCl	0.28 ± 0.03	0.93 ± 0.23	-0.20 ± 0.04	-0.13 ± 0.02	0.19 ± 0.04	2065 ± 115	-36.0 ± 0.1	-35.9 ± 0.1
NaCl	0.38 ± 0.07	0.79 ± 0.15	-0.19 ± 0.06	-0.10 ± 0.03	0.11 ± 0.06	448 ± 136	-32.2 ± 0.8	-32.0 ± 0.8
$CaCl_2$	0.34 ± 0.02	0.55 ± 0.06	-0.15 ± 0.04	-0.05 ± 0.02	0.06 ± 0.03	354 ± 53	-31.7 ± 0.4	-31.5 ± 0.4
$MgCl_2$	0.44 ± 0.02	0.64 ± 0.03	-0.62 ± 0.06	-0.12 ± 0.01	0.05 ± 0.01	2753 ± 186	-36.8 ± 0.2	-36.1 ± 0.2
NaOAc	0.39 ± 0.05	0.78 ± 0.13	-0.81 ± 0.09	-0.33 ± 0.05	0.10 ± 0.03	586 ± 198	-32.8 ± 1.0	-32.0 ± 1.0
$NaNO_3$	0.29 ± 0.07	0.48 ± 0.03	0.34 ± 0.04	-0.39 ± 0.06	0.26 ± 0.04	1646 ± 371	-35.4 ± 0.6	-35.8 ± 0.6
No Salt	0.36 ± 0.03	0.63 ± 0.04	-1.08 ± 0.03	-0.35 ± 0.07	0.08 ± 0.02	1458 ± 443	-35.1 ± 0.7	-34.0 ± 0.8

As can be seen from the Table 4.1, enthalpy values are exothermic and quite smaller than the literature values of complexation of HA and CHI with other molecules (HA-BSA and HA-BLG[22], chitosan-sodium alginate[61], chitosan-gum arabic [62]). This fact is also valid when we compare the results of our previous work [54] regarding the thermodynamics of HA-CHI mixture. The enthalpy value for ion-pairing (ΔH_{IP}) was found as 0.83 kJ/mol in acetate buffer/NaCl solution with I_{total} = 0.05 M at pH = 4.0.[54] The enthalpy value is endothermic and - it is four times greater in magnitude than ΔH_{IP} of -0.19 kJ/mol in citric acid buffer/NaCl solution.

Considering the results from the potentiometric titration that HA chains are 26 ± 0.02 % charged, and CHI chains are 99 ± 0.1 % charged at pH = 3.25, these two polyelectrolytes do not have charge complementarity with each other, which can be the reason for the smaller enthalpy values. On the other hand, HA is 90% charged whereas CHI is estimated as fully charged at pH = 4.0 in 0.15 M, which indicates a higher charge complementarity in our previous study [54] and therefore higher ΔH_{IP} values. Meanwhile, there are also studies showing quite small enthalpy of complexation values for polyelectrolyte complexes, as in our study. For instance, enthalpy of ion pairing process

between potassium poly(3-sulfopropylmethacrylate) (PSPMA) and poly(2-methacryloxy)ethyl)trimethylammonium chloride) (PMETAC) found as -0.4 kJ/mol at pH = 2.0 [63]. In another study, the enthalpy values of complex coacervation formation of poly(L-orthine hydrobromide) (PO) and poly(L-glutamic acid sodium salt) (PGlu) mixture change between 0.01 to 0.26 kJ/mol for the different salt concentrations within 0-800 mM.[9]

Moreover, having negative Gibbs free energy values shown in Table 4.1, the interactions between the oppositely charged HA and CHI were found to be spontaneous. Additionally, it is the entropic contribution ($T\Delta S_{IP}$= 31.5 – 36.1 kJ/mol) that has greater impact on Gibbs free energy than that of enthalpy values (ΔH_{IP} ranges from -0.15 to -1.08 kJ/mol), showing entropically driven process. Our findings align with the results of the our previous study with HA and CHI mixtures having significantly larger $T\Delta S_{IP}$ values (29.3 kJ/mol) than the ΔH_{IP} values (0.83 kJ/mol) in acetate buffer/NaCl solution with I_{total} = 0.05 M at pH = 4.0 [54]. Additionally, another study with ion pairing entropy ($T\Delta S_1$= 17.2 – 29.2 kJ/mol) and enthalpy of ion-pairing (ΔH_1= -1.9 – 0.9 kJ/mol) shows the domination of entropic contribution for the PSPMA- PMETAC complexation. [63]

When the entropic contributions ($T\Delta S_{IP}$) of the ion-pairing are compared, the values are all positive, and the magnitude is ordered as follows: $Mg^{2+} > K^+ > Na^+ > Ca^{2+}$ and $NO_3^- > OAc^- = Cl^-$. According to these results, the following interpretation can be made: Ions with higher hydration energy are expected to interact more with water molecules than the polyelectrolyte, decreasing the hydration of the polyelectrolyte. Thus, the interaction between less hydrated charged groups on the polyelectrolyte chains with water molecules is weaker, and polyelectrolyte-polyelectrolyte interactions increased where the release of counterions contributes to the higher entropy.

The salt ions screen the charges on the polymers at higher concentrations, whereas the addition of small amounts of salt can promote the interactions between the oppositely charged polymers. This behavior is observed in a study where the formation of the poly(acrylic acid sodium salt) (pAA)- poly(allylamine hydrochloride) (pAH) complex is promoted, showing higher turbidity up to a certain level of salt concentration, in which further addition (≥75 mM) diminished the interactions between the two polyelectrolytes, indicated by a decrease in turbidity [24]. In this regard, our data suggest that salt-free

condition (no salt, only buffer without any added salt) shows the most negative enthalpy values demonstrating the stronger interaction between HA-CHI, compared to the presence of added salts.

When enthalpy values of monovalent and divalent cations are compared, it is observed that Na^+ and K^+ show closely matching enthalpy values. Our finding is in accordance with the previously mentioned study done by Oppermann and Schulz [36] that the enthalpy of complexation between two oppositely charged polyelectrolytes (PSS and PTMA) showed less change with monovalent cations. Their results also demonstrate that enthalpy of complexation in the presence of Mg^{2+} and Ca^{2+} exhibit minimal difference. Considering our results, however, the enthalpy of complexation is more exothermic for Mg^{2+} than that of Ca^{2+}.

The standard molar enthalpies of hydration ($-\Delta H_{hyd}$) of the selected ions in this study follows this order for cations $Mg^{2+} > Ca^{2+} > Na^+ > K^+$ and $OAc^- > Cl^- > NO_3^-$ for the anions [64].The hydration energy, aka. hydration enthalpy, defined as the amount of energy release when ion is solvated by water molecules and it is positively correlated with the ion charge density. Charge density of the ions (=ion charge x electron charge / volume of ion) follows the similar trend with the hydration energy.[65] Thus, more exothermic hydration shows that salting-out is particularly pronounced for the ions with high charge density.[66]. Being more hydrated, kosmotropic ions are expected to interact more with water molecules than the polyelectrolyte. Their tendency of salting out decreases the solubility of the polyelectrolyte, favoring phase separation. However, in the presence of the less hydrated ions, the phase separation is expected to be disfavored by salting in behavior[24]. That's why the interaction between the HA-CHI is expected to be more favorable in the presence of kosmotropes. When comparing the results of the anions in Table 4.1, it is the OAc^- ion condition that shows more exothermic enthalpy values compared to NO_3^- and Cl^-. Therefore, from these results, the following interpretation can be proposed: Ions having a higher charge density result in stronger attractions between the water molecules and the kosmotropic ions in the solution, releasing more energy when they are hydrated, making ΔH_{IP} more exothermic. Thus, more negative enthalpy of hydration values for the ions (strong affinity for water molecules) help facilitate the HA-CHI interactions, leading to the coacervation process. This observation is aligned with the studies done by Perry et al. and Fu et al.[1, 24] The former study showed that kosmotropic

CH_3COO^- showed higher critical salt concentration, the point at which further addition diminished the interactions between the two polyelectrolytes, compared to Cl^- and NO_3^-. They discussed that polymer solubility is decreased due to the kosmotropic tendency of the acetate ion thus favoring phase separation. In the latter study more exothermic complexation enthalpy is found for the more hydrated anions such as Ac^- (ΔH_{PEC}= -3.45 kJ/mol) compared to Cl^- and NO_3^- (ΔH_{PEC}= -1.87 kJ/mol and ΔH_{PEC}= -2.21 kJ/mol, respectively), as it was in our case.

5. CONCLUSION

In this study, the formation of complex coacervation between two oppositely charged polyelectrolytes, hyaluronic acid (HA) and chitosan (CHI), was investigated with respect to the specific ion effects of NaCl, KCl, $CaCl_2$, $MgCl_2$, $NaNO_3$, and NaOAc salts at acidic pH. The fundamental aim is to investigate the specific ion effects on the thermodynamics of the system.

Turbidimetric titration experiments revealed that the order follows the Hofmeister series, with higher turbidity of kosmotropic cations except that Ca^{+2} comes after Mg^{+2}. The order of the turbidity values for the anions found to be more complex. Although, there is no significant difference found for the droplet diameters measured at the highest molar ratio, a higher number of droplets were observed via light microscopy at the higher molar ratios. Moreover, at pH = 3.25, CHI is found to be nearly fully charged (99 ± 0.01 %) whereas HA is less charged (26 ± 0.02 %) in comparison by potentiometric titration.

The thermodynamic parameters from fitted ITC data by two-step model showed exothermic enthalpy values and entropic contribution ($T\Delta S_{IP}$) having a greater impact on Gibbs free energy than that of enthalpy values of ion pairing (ΔH_{IP}). The $T\Delta S_{IP}$ of cations follows the same order as their ΔH_{IP} (Mg^{2+} > K^{+} > Na^{+} > Ca^{2+}) however, anions followed different order as NO_3^- > OAc^- = Cl^-.

Finally, the salt-screening effect of the ions is evident, thus salt-free condition shows the most negative enthalpy values demonstrating the stronger interaction between HA-CHI, compared to the presence of added salts. Enthalpy values showed less change with monovalent cations. However, the enthalpy of complexation found as more exothermic for Mg^{2+} than that of Ca^{2+}. OAc^- ion condition that shows more exothermic enthalpy values compared to NO_3^- and Cl^-. Thus, ions with higher charge density help facilitate the HA-CHI interactions, making ΔH_{IP} more exothermic.

REFERENCES

1. Fu, J. and J.B. Schlenoff, "Driving Forces for Oppositely Charged Polyion Association in Aqueous Solutions: Enthalpic, Entropic, but Not Electrostatic", *Journal of the American Chemical Society,* Vol. 138, No. 3, pp. 980-90, 2016.
2. van der Gucht, J., E. Spruijt, M. Lemmers, and M.A. Cohen Stuart, "Polyelectrolyte Complexes: Bulk Phases and Colloidal Systems", *Journal of Colloid and Interface Science,* Vol. 361, No. 2, pp. 407-22, 2011.
3. Jong, H.G. and H.R. Kruyt, "Coacervation (Partial Miscibility in Colloid Systems)", *Proceedings of the Koninklijke Nederlandse Akademie van Wetenschappen,* Vol. 32, pp. 849-856, 1929.
4. De Jong, H.B. and H. Kruyt, "Colloid Science", *R. Kruyt (ed.), Elsevier, Amsterdam,* 1949.
5. Oparin, A.I., "The Origin of Life and the Origin of Enzymes", *Advances in Enzymology and Related Areas of Molecular Biology,* Vol. 27, pp. 347-80, 1965.
6. Kizilay, E., A.B. Kayitmazer, and P.L. Dubin, "Complexation and Coacervation of Polyelectrolytes with Oppositely Charged Colloids", *Advances in Colloid and Interface Science,* Vol. 167, No. 1-2, pp. 24-37, 2011.
7. Zhou, L., H. Shi, Z. Li, and C. He, "Recent Advances in Complex Coacervation Design from Macromolecular Assemblies and Emerging Applications", *Macromolecular Rapid Communications,* Vol. 41, No. 21, p. 2000149, 2020.
8. Timilsena, Y.P., T.O. Akanbi, N. Khalid, B. Adhikari, and C.J. Barrow, "Complex Coacervation: Principles, Mechanisms and Applications in Microencapsulation", *International Journal of Biological Macromolecules,* Vol. 121, pp. 1276-1286, 2019.
9. Priftis, D., N. Laugel, and M. Tirrell, "Thermodynamic Characterization of Polypeptide Complex Coacervation", *Langmuir,* Vol. 28, No. 45, pp. 15947-15957, 2012.
10. Kayitmazer, A.B., "Thermodynamics of Complex Coacervation", *Advances in Colloid and Interface Science,* Vol. 239, pp. 169-177, 2017.

11. Yang, M., S.L. Sonawane, Z.A. Digby, J.G. Park, and J.B. Schlenoff, "Influence of “Hydrophobicity” on the Composition and Dynamics of Polyelectrolyte Complex Coacervates", *Macromolecules,* Vol. 55, No. 17, pp. 7594-7604, 2022.
12. Muhoza, B., S. Xia, X. Wang, X. Zhang, Y. Li, and S. Zhang, "Microencapsulation of Essential Oils by Complex Coacervation Method: Preparation, Thermal Stability, Release Properties and Applications", *Critical Reviews in Food Science and Nutrition,* Vol. 62, No. 5, pp. 1363-1382, 2022.
13. Devi, N., M. Sarmah, B. Khatun, and T. Maji, "Encapsulation of Active Ingredients in Polysaccharide-Protein Complex Coacervates", *Advances in Colloid and Interface Science,* Vol. 239, pp. 136-145, 2017.
14. McTigue, W.B. and S. Perry, "Design Rules for Encapsulating Proteins into Complex Coacervates", *Soft Matter,* Vol. 15, No. 15, pp. 3089-3103, 2019.
15. Xu, Y., M. Mazzawi, K. Chen, L. Sun, and P. Dubin, "Protein Purification by Polyelectrolyte Coacervation: Influence of Protein Charge Anisotropy on Selectivity", *Biomacromolecules,* Vol. 12, No. 5, pp. 1512-1522, 2011.
16. Peng, Q., J. Chen, Z. Zeng, T. Wang, L. Xiang, X. Peng, J. Liu, and H. Zeng, "Adhesive Coacervates Driven by Hydrogen-Bonding Interaction", *Small,* Vol. 16, No. 43, p. 2004132, 2020.
17. Johnson, N. and Y. Wang, "Coacervate Delivery Systems for Proteins and Small Molecule Drugs", *Expert Opinion on Drug Delivery,* Vol. 11, pp. 1829-1832, 2014.
18. Ma, L., X. Fang, and C. Wang, "Peptide-based Coacervates in Therapeutic Applications", *Frontiers in Bioengineering and Biotechnology,* Vol. 10, 2023.
19. Vahdati, M., F.J. Cedano-Serrano, C. Creton, and D. Hourdet, "Coacervate-Based Underwater Adhesives in Physiological Conditions", *ACS Applied Polymer Materials,* Vol. 2, No. 8, pp. 3397-3410, 2020.
20. Khoonkari, M., J. Es Sayed, M. Oggioni, A. Amirsadeghi, P. Dijkstra, D. Parisi, F. Kruyt, P. Van Rijn, M.K. Włodarczyk-Biegun, and M. Kamperman, "Bioinspired Processing: Complex Coacervates as Versatile Inks for 3D Bioprinting", *Advanced Materials,* Vol. 35, No. 28, p. 2210769, 2023.
21. Kayitmazer, A.B., A.F. Koksal, and E. Kilic Iyilik, "Complex Coacervation of Hyaluronic Acid and Chitosan: Effects of pH, Ionic Strength, Charge Density, Chain Length and the Charge Ratio", *Soft Matter,* Vol. 11, No. 44, pp. 8605-8612, 2015.

22. Du, X., P.L. Dubin, D.A. Hoagland, and L. Sun, "Protein-Selective Coacervation with Hyaluronic Acid", *Biomacromolecules,* Vol. 15, No. 3, pp. 726-734, 2014.
23. Soussi Hachfi, R., P. Hamon, F. Rousseau, M.-H. Famelart, and S. Bouhallab, "Ionic Strength Dependence of the Complex Coacervation between Lactoferrin and β-Lactoglobulin", *Foods,* Vol. 12, No. 5, p. 1040, 2023.
24. Perry, S., Y. Li, D. Priftis, L. Leon, and M. Tirrell, "The Effect of Salt on the Complex Coacervation of Vinyl Polyelectrolytes", *Polymers,* Vol. 6, No. 6, pp. 1756-1772, 2014.
25. Jungwirth, P. and P.S. Cremer, "Beyond Hofmeister", *Nature Chemistry,* Vol. 6, No. 4, pp. 261-263, 2014.
26. Hofmeister, F., "Zur Lehre von der Wirkung der Salze", *Archiv für Experimentelle Pathologie und Pharmakologie,* Vol. 25, No. 1, pp. 1-30, 1888.
27. Lo Nostro, P. and B.W. Ninham, "Hofmeister Phenomena: An Update on Ion Specificity in Biology", *Chemical reviews,* Vol. 112, No. 4, pp. 2286-2322, 2012.
28. Jaspers, M., A.E. Rowan, and P.H. Kouwer, "Tuning Hydrogel Mechanics Using the Hofmeister Effect", *Advanced Functional Materials,* Vol. 25, No. 41, pp. 6503-6510, 2015.
29. Musilová, L., V. Kašpárková, A. Mráček, A. Minařík, and M. Minařík, "The Behaviour of Hyaluronan Solutions in the Presence of Hofmeister Ions: A Light Scattering, Viscometry and Surface Tension Study", *Carbohydrate Polymers,* Vol. 212, pp. 395-402, 2019.
30. Salis, A. and B.W. Ninham, "Models and Mechanisms of Hofmeister Effects in Electrolyte Solutions, and Colloid and Protein Systems Revisited", *Chemical Society Reviews,* Vol. 43, No. 21, pp. 7358-7377, 2014.
31. Gregory, K.P., G.R. Elliott, H. Robertson, A. Kumar, E.J. Wanless, G.B. Webber, V.S.J. Craig, G.G. Andersson, and A.J. Page, "Understanding Specific Ion Effects and the Hofmeister Series", *Physical Chemistry Chemical Physics,* Vol. 24, No. 21, pp. 12682-12718, 2022.
32. Mazzini, V. and V.S.J. Craig, "What Is the Fundamental Ion-specific Series for Anions and Cations? Ion Specificity in Standard Partial Molar Volumes of Electrolytes and Electrostriction in Water and Non-aqueous Solvents", *Chemical Science,* Vol. 8, No. 10, pp. 7052-7065, 2017.

33. Zhang, Y. and P.S. Cremer, "Interactions Between Macromolecules and Ions: The Hofmeister Series", *Current Opinion in Chemical Biology,* Vol. 10, No. 6, pp. 658-63, 2006.
34. Kang, B., H. Tang, Z. Zhao, and S. Song, "Hofmeister Series: Insights of Ion Specificity from Amphiphilic Assembly and Interface Property", *ACS Omega,* Vol. 5, No. 12, pp. 6229-6239, 2020.
35. Das, S. and S. Majumdar, "Competitive Effects of Anion Mobility and Viscous Forces on the Interactions of Hyaluronic Acid and Alginic Acid with Hofmeister Salts", *Food Hydrocolloids,* Vol. 159, p. 110684, 2025.
36. Oppermann, W. and T. Schulz, "Interaction Between Oppositely Charged Polyelectrolytes in Aqueous Solution", *Makromolekulare Chemie. Macromolecular Symposia,* Vol. 39, No. 1, pp. 293-299, 1990.
37. Zhang, Y. and P.S. Cremer, "The Inverse and Direct Hofmeister Series for Lysozyme", *Proceedings of the National Academy of Sciences of the United States of America,* Vol. 106, No. 36, pp. 15249-53, 2009.
38. Tatini, D., F. Sarri, P. Maltoni, M. Ambrosi, E. Carretti, B.W. Ninham, and P. Lo Nostro, "Specific Ion Effects in Polysaccharide Dispersions", *Carbohydrate Polymers,* Vol. 173, pp. 344-352, 2017.
39. Das, S. and S. Majumdar, "Enhancing the Properties of Self-Healing Gelatin Alginate Hydrogels by Hofmeister Mediated Electrostatic Effect", *ChemPhysChem,* Vol. 25, No. 1, p. e202300660, 2024.
40. Zhu, L., Y. Pan, Z. Hua, Y. Liu, and X. Zhang, "Ionic Effect on the Microenvironment of Biomolecular Condensates", *Journal of the American Chemical Society,* Vol. 146, No. 20, pp. 14307-14317, 2024.
41. Aranaz, I., A.R. Alcántara, M.C. Civera, C. Arias, B. Elorza, A. Heras Caballero, and N. Acosta, "Chitosan: An Overview of Its Properties and Applications", *Polymers,* Vol. 13, No. 19, p. 3256, 2021.
42. Iamsamai, C., S. Hannongbua, U. Ruktanonchai, A. Soottitantawat, and S.T. Dubas, "The Effect of the Degree of Deacetylation of Chitosan on Its Dispersion of Carbon Nanotubes", *Carbon,* Vol. 48, No. 1, pp. 25-30, 2010.
43. Kiang, T., J. Wen, H.W. Lim, and K.W. Leong, "The Effect of the Degree of Chitosan Deacetylation on the Efficiency of Gene Transfection", *Biomaterials,* Vol. 25, No. 22, pp. 5293-5301, 2004.

44. Jayakumar, R., D. Menon, M. Koyakutty, S.V. Nair, and H. Tamura, "Biomedical Applications of Chitin and Chitosan Based Nanomaterials—A Short Review", *Carbohydrate Polymers,* Vol. 82, No. 2, pp. 227-232, 2010.

45. Lastra, M.L., M.S. Molinuevo, A.M. Cortizo, and M.S. Cortizo, "Fumarate Copolymer–Chitosan Cross-Linked Scaffold Directed to Osteochondrogenic Tissue Engineering", *Macromolecular Bioscience,* Vol. 17, No. 5, 2017.

46. Oh, E.J., K.E. Park, K.S. Kim, J. Kim, J. Yang, J.-H. Kong, M.Y. Lee, A.S. Hoffman, and S.K. Hahn, "Target Specific and Long-Acting Delivery of Protein, Peptide, and Nucleotide Therapeutics Using Hyaluronic Acid Derivatives", *Journal of Controlled Release : Official Journal of The Controlled Release Society,* Vol. 141, No. 1, pp. 2-12, 2010.

47. Maiz-Fernández, S., N. Barroso, L. Pérez-Álvarez, U. Silván, J.L. Vilas-Vilela, and S. Lanceros-Mendez, "3D Printable Self-Healing Hyaluronic Acid/Chitosan Polycomplex Hydrogels with Drug Release Capability", *International Journal of Biological Macromolecules,* Vol. 188, pp. 820-832, 2021.

48. Wiseman, T., S. Williston, J.F. Brandts, and L.-N. Lin, "Rapid Measurement of Binding Constants and Heats of Binding Using a New Titration Calorimeter", *Analytical Biochemistry,* Vol. 179, No. 1, pp. 131-137, 1989.

49. Pierce, M.M., C.S. Raman, and B.T. Nall, "Isothermal Titration Calorimetry of Protein–Protein Interactions", *Methods,* Vol. 19, No. 2, pp. 213-221, 1999.

50. Misra, G., *Data Processing Handbook for Complex Biological Data Sources*, Academic Press, San Diego, 2019.

51. Rajarathnam, K. and J. Rösgen, "Isothermal Titration Calorimetry of Membrane Proteins — Progress and Challenges", *Biochimica et Biophysica Acta (BBA) - Biomembranes,* Vol. 1838, No. 1, Part A, pp. 69-77, 2014.

52. Vitorazi, L., N. Ould-Moussa, S. Sekar, J. Fresnais, W. Loh, J.P. Chapel, and J.F. Berret, "Evidence of a Two-Step Process and Pathway Dependency in the Thermodynamics of Poly(Diallyldimethylammonium Chloride)/Poly(Sodium Acrylate) Complexation", *Soft Matter,* Vol. 10, No. 47, pp. 9496-9505, 2014.

53. Dos Santos De Macedo, B., T. De Almeida, R. Da Costa Cruz, A.D.P. Netto, L. Da Silva, J.-F. Berret, and L. Vitorazi, "Effect of pH on the Complex Coacervation and on the Formation of Layers of Sodium Alginate and PDADMAC", *Langmuir,* Vol. 36, No. 10, pp. 2510-2523, 2020.

54. Akcay Ogur, F., S. Mamasoglu, S.L. Perry, F.A. Akin, and A.B. Kayitmazer, "Interactions between Hyaluronic Acid and Chitosan by Isothermal Titration Calorimetry: The Effect of Ionic Strength, pH, and Polymer Molecular Weight", *The Journal of Physical Chemistry B,* Vol. 128, No. 37, pp. 9022-9035, 2024.
55. Yang, M., Z.A. Digby, and J.B. Schlenoff, "Precision Doping of Polyelectrolyte Complexes: Insight on the Role of Ions", *Macromolecules,* Vol. 53, No. 13, pp. 5465-5474, 2020.
56. Kantarci, G., S. Mamasoglu, and A.B. Kayitmazer, "The Effect of Hofmeister Ions on Thermodynamics of Complex Coacervation Between Hyaluronic Acid and Chitosan ", ChemRxiv: chemrxiv-2023-5bq6r-v2, 2023.
57. Kantarci, G., *Effect of Hofmeister Ions on Thermodynamics of Complex Coacervation of Hyaluronic Acid and Chitosan*, M.S. Thesis, Boğaziçi University, 2022.
58. Qin, C., H. Li, Q. Xiao, Y. Liu, J. Zhu, and Y. Du, "Water-Solubility of Chitosan and Its Antimicrobial Activity", *Carbohydrate Polymers,* Vol. 63, No. 3, pp. 367-374, 2006.
59. Bates, R.G. and G.D. Pinching, "Resolution of the Dissociation Constants of Citric Acid at 0 to 50°, and Determination of Certain Related Thermodynamic Functions", *Journal of the American Chemical Society,* Vol. 71, No. 4, pp. 1274-1283, 1949.
60. Yamazaki, M., M. Yabe, and K. Iijima, "Specific Ion Effects on the Aggregation of Polysaccharide-based Polyelectrolyte Complex Particles Induced by Monovalent Ions within Hofmeister Series", *Journal of Colloid and Interface Science,* Vol. 643, pp. 305-317, 2023.
61. Yilmaz, T., L. Maldonado, H. Turasan, and J. Kokini, "Thermodynamic Mechanism of Particulation of Sodium Alginate and Chitosan Polyelectrolyte Complexes as a Function of Charge Ratio and Order of Addition", *Journal of Food Engineering,* Vol. 254, pp. 42-50, 2019.
62. Vuillemin, M.E., F. Michaux, L. Muniglia, M. Linder, and J. Jasniewski, "Gum Arabic and Chitosan Self-Assembly: Thermodynamic and Mechanism Aspects", *Food Hydrocolloids,* Vol. 96, pp. 463-474, 2019.
63. Yuan, H. and G. Liu, "Polyelectrolyte Complexation When Considering the Counterion-Mediated Hydrogen Bonding", *Langmuir,* Vol. 38, No. 26, pp. 8179-8186, 2022.

64. Yizhak, M., *Ion Solvation in Neat Solvents*, John Wiley & Sons, New Jersey, 2015.

65. Rayner-Canham, G., G. Rayner-Canham, and T. Overton, *Descriptive Inorganic Chemistry*, W. H. Freeman, New York, 2009.

66. Hyde, A.M., S.L. Zultanski, J.H. Waldman, Y.-L. Zhong, M. Shevlin, and F. Peng, "General Principles and Strategies for Salting-Out Informed by the Hofmeister Series", *Organic Process Research & Development,* Vol. 21, No. 9, pp. 1355-1370, 2017.

APPENDIX A: SUPPLEMENTARY DATA

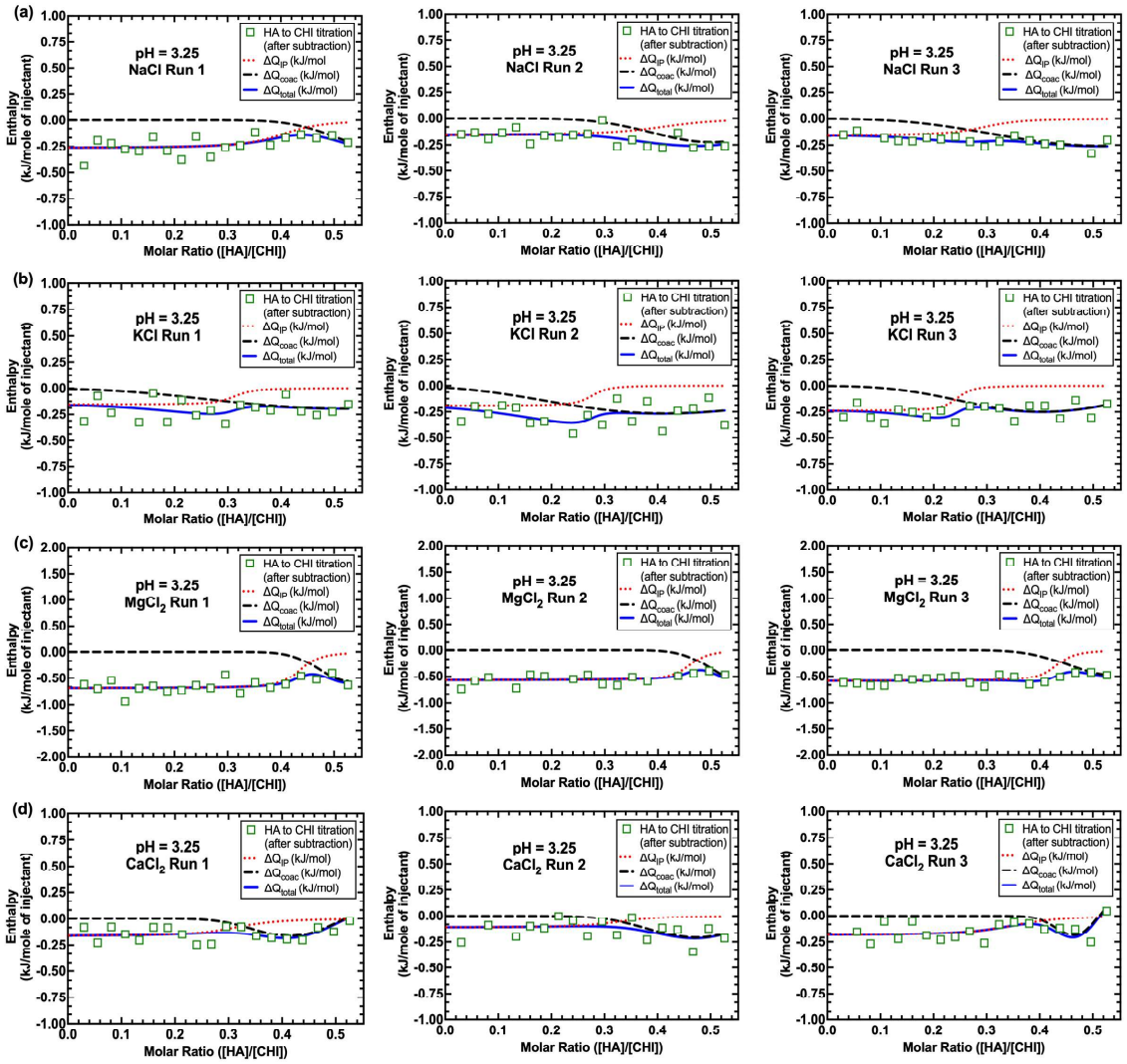

Figure A.1. Enthalpy versus molar ratio ([HA]/[CHI]) plots at pH = 3.25 for (a) NaCl, (b) KCl, (c) $MgCl_2$, (d) $CaCl_2$. T = 25°C.

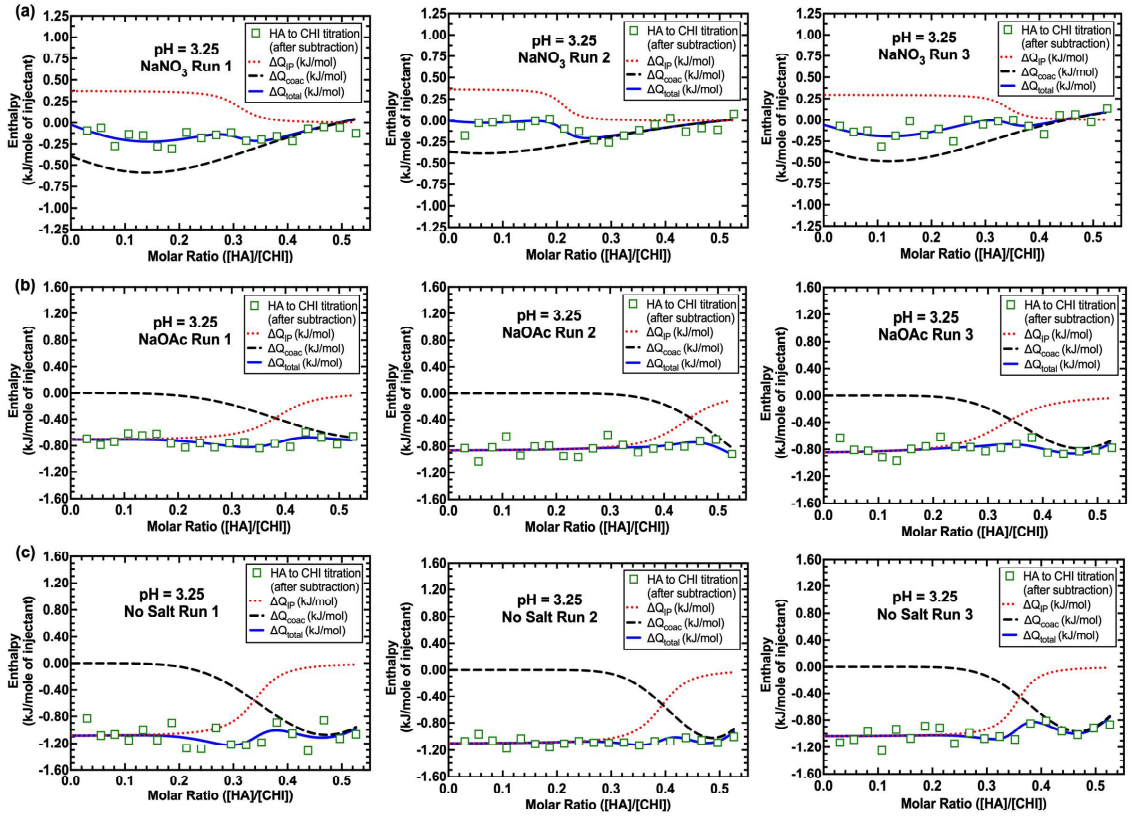

Figure A. 2. Enthalpy versus molar ratio ([HA]/[CHI]) plots at pH = 3.25 for (a) $NaNO_3$, (b) NaOAc, (c) No salt. T = 25°C.